

Cobalt and Nitrogen Co-doped Porous Carbon Spheres as Efficient Oxygen Reduction Electrocatalysts

Hanzeng Zou¹, Zhaoyan Chen¹, Xia Xiong¹, Yueyang Sun¹, Supeng Pei^{1,*}, Yongming Zhang^{2,3}

¹ School of Chemical and Environmental Engineering, Shanghai Institute of Technology, Shanghai 201418, China.

² School of Chemistry and Chemical Engineering, Shanghai Jiao Tong University, Shanghai 200240, China.

³ State Key Laboratory of Fluorinated Functional Membrane Materials, China.

*E-mail: peisupeng@126.com

Received: 6 October 2019 / Accepted: 18 December 2019 / Published: 10 February 2020

In this paper, cobalt and nitrogen co-doped carbon sphere catalysts were synthesized by two methods, electrospinning and grinding. The two kinds of Co,N co-doped carbon sphere catalysts were compared in a system. According to the results, Co-N-C-37.5 catalyst has a better oxygen reduction reaction (ORR) performance and a more spherical shape than the other catalysts. Additionally, it has the largest specific surface area of all tested electrocatalysts. For the electrochemical activity, the onset potential (E_{onset}) of Co-N-C-37.5 is 0.979 V, which is better than that of the commercial Pt/C catalyst (0.967 V). The half-wave potential ($E_{1/2}$) of Co-N-C-37.5 is 0.780 V, which is slightly lower than that of the commercial Pt/C (0.797 V). After 10,000 s of durability testing, 88% of current is retained with Co-N-C-37.5, which is better than that of commercial Pt/C (83%). In addition, the methanol tolerance of Co-N-C-37.5 is better than that of the commercial Pt/C. The current density percentage of Co-N-C-37.5 has no distinct decrease after the addition of methanol at 500 s. However, the commercial Pt/C decreases sharply. Therefore, this study provides a facile way to produce Co, N co-doped carbon sphere catalysts with good catalytic performance for the ORR.

Keywords: Electrospinning; Co, N co-doped; Carbon sphere; Oxygen reduction reaction

1. INTRODUCTION

With the excessive consumption of fossil energy and global climate change caused by the emission of greenhouse gas, much effort has been devoted to developing environmentally friendly devices[1-5]. Among these devices, fuel cells have drawn a great deal of attention, especially proton exchange membrane fuel cells (PEMFCs), which could directly convert chemical energy to electrical energy. PEMFCs have many advantages, such as a high energy conversion rate and high energy

density, and high energy density; furthermore, they are highly reliable and operate at low working temperatures[6]. However, several challenges hinder the large-scale commercialization of PEMFCs; they have poor long-term stability and a larger loading of platinum (Pt) and Pt-based catalysts, which are expensive[7-10]. Among these obstacles, the high costs of platinum (Pt) and Pt-based catalysts are the most serious problem. When Jasinsky discovered that cobalt phthalocyanine, a metal macrocyclic compound, had good oxygen reduction reaction activity in 1964[11], a large number of researchers began to use non-noble metal catalysts (M-N-C) instead of Pt-based ORR catalysts.

Although non-precious metals (such as Fe, Co, Ni, Cu and Mn) and heteroatoms (such as N, F, P and S) can be co-doped on carbon supports, the active sites of the ORR catalysts and the reaction mechanism are unclear[12]. It is universally acknowledged that cobalt (Co) and nitrogen (N) co-doped carbon nanomaterials have better oxygen reduction reaction catalytic performance and stability than other non-noble metal catalysts[13-15]. In addition, the specific surface area of the catalysts is also a pivotal key to affecting the ORR activity of the catalysts, because additional active sites can be provided by a large specific surface area, which can effectively accelerating the contact of O₂ and electrolyte and then to the benefitting the ORR.

For these reasons, we intend to introduce cobalt into the nitrogen-doped mesoporous carbon spheres. Two kinds of Co, N co-doped carbon sphere catalysts were compared in a system. Then, the relationship between the ORR performance and the morphologies and structures of the catalysts was studied in this paper.

2. EXPERIMENTAL DETAIL

2.1 Materials

Polyacrylonitrile (PAN, Mw ~150,000 g/mol), polyvinylpyrrolidone (PVP, Mw ~5,500 g/mol), and fumed silica (particle size are about 35 nm) were purchased from J&K, Shanghai Qifu Materials Tech Co., Ltd, and Jilin Shuangji Chemical New Materials Tech Co., Ltd, respectively. Dimethylformamide (DMF), hydrofluoric acid (HF), and cobalt acetate tetrahydrate (Co(Ac)₂·4H₂O) were purchased from Sinopharm Chemical Reagent Co., Ltd.

2.2 Synthesis of Co-N-C-x and Co@N-C-37.5 spheres electrocatalyst

In a typical procedure, 37.5 mg of cobalt acetate tetrahydrate, 0.43 g of fumed silica, 0.50 g of PVP and 0.50 g of PAN were added in 9 g of DMF solution under magnetic stirring for 24 h to gain an electrospinning solution. The electrospinning working voltage was 12 kV, the working distance was 15 cm, and the solution flow rate was 0.05 ml h⁻¹ with a temperature and the relative humidity of 28 °C and 38%, respectively. The electrospinning fiber was placed on an Al foil as the collector.

The prepared polymer spheres were preoxidized in a furnace at 220 °C in an O₂ atmosphere for 100 min with a heating rate of 2 °C min⁻¹ and kept at the final temperature for 120 min. Then, the polymer spheres were heated at 800 °C for 390 min under a N₂ flow and kept at the final temperature

for 2 h. Next, the catalyst was etched by HF for 6 h and washed for several times with deionized water. Finally, the catalyst was dried at 60 °C in the vacuum oven for 12 h. The catalyst was named as Co-N-C-37.5 (37.5 was the weight of cobalt acetate tetrahydrate). In addition, x in Co-N-C-x means that the mass of cobalt acetate tetrahydrate was added in the solution.

For comparison, N-C (without cobalt acetate tetrahydrate), Co-N-C-18.75, Co-N-C-56.25, Co-N-C-75 spheres catalysts were fabricated in the same manner. Co@N-C-37.5 was fabricated by grinding method. A certain amount of cobalt acetate tetrahydrate was ground on the prepared N-C spheres which were only preoxidized (the concentration of cobalt acetate tetrahydrate in the Co@N-C-37.5 was the same in Co-N-C-37.5). The catalyst was named as Co@N-C-37.5.

2.3 Physical characteristics

The SEM images were gained by the JEOL2100F scanning electron microscopy. An X-ray diffraction test was carried out by an APLX-DUO instrument with Cu K α radiation ($\lambda=1.5418 \text{ \AA}$). X-ray photoelectron spectroscopy (XPS) was conducted on the AXIS UltraDLD X-ray photoelectron spectrometer with Al K α radiation. Raman spectra was carried out on the Thermo Fisher H31XYZE-US equipment with a laser source of 532 nm. Specific surface area was measured by an ASAP-2460 instrument under N₂ and then calculated by N₂ adsorption and desorption isotherms through the Brunauer-Emmett-Teller (BET) method. The pore size distributions of the catalysts were calculated by N₂ adsorption isotherms using the Barrett–Joyner–Halenda (BJH) model.

2.4 Electrochemical measurements

The cyclic voltammetry (CV) test, linear sweep voltammetry (LSV) test, durability test and methanol tolerance test were conducted with an Autolab PGSTAT302 (Metrohm) instrument through a three-electrode system with a glassy carbon (GC) electrode as the working electrode, Pt wire as the counter electrode, and Ag/AgCl (3.0 M KCl) as the reference electrode. In addition, LSV rotation speed ranges from 400 to 2000 rpm at a scan rate of 10 mV s⁻¹. The durability test and methanol tolerance (3M CH₃OH) tests were conducted by measuring the chronoamperometric response under 0.35 V at 1600 rpm. After testing, the Ag/AgCl electrode was calibrated with the reversible hydrogen electrode (RHE), the potentials were converted using an equation[16]:

$$E \text{ (vs. RHE)} = E_{\text{Ag/AgCl}} + \text{pH} \times 0.059 + 0.210 \quad (1)$$

To further clarify the electron transfer number of the reaction, the Koutecky-Levich (K-L) equation are listed as followed:

$$\frac{1}{J} = \frac{1}{J_L} + \frac{1}{J_k} = \frac{1}{B\omega^{1/2}} + \frac{1}{J_k} \quad (2)$$

$$J_k = nFkC_0 \quad (3)$$

$$B = 0.2nFC_0(D_0)^{2/3}v^{-1/6}J_k = nFkC_0 \quad (4)$$

J is the measured current density, J_k and J_L are the kinetic and limiting current densities, respectively. n is the electron transfer number, F is the Faraday constant (96,485 C mol⁻¹), C₀ is the

bulk concentration of O_2 ($1.2 \times 10^{-6} \text{ mol cm}^{-3}$), D_0 is the diffusion coefficient of O_2 in electrolytes ($1.9 \times 10^{-5} \text{ cm}^2 \text{ s}^{-1}$), ν is the kinematic viscosity of the electrolyte ($0.01 \text{ cm}^2 \text{ s}^{-1}$) and k is the electron-transfer rate constant. A coefficient of 0.2 is adopted when the unit of rotational speed is rpm.

3. RESULTS AND DISCUSSION

As illustrated in Fig. 1, the Co-N-C spheres were fabricated via electrospinning the solution that contained silica as hard templates. Then, the samples were preoxidized at 220 °C and carbonized at 800 °C.

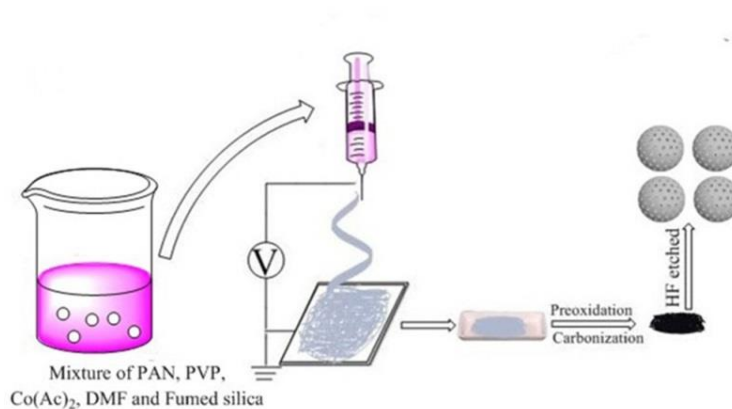


Figure 1. Schematic representation for the preparation of the electrocatalysts

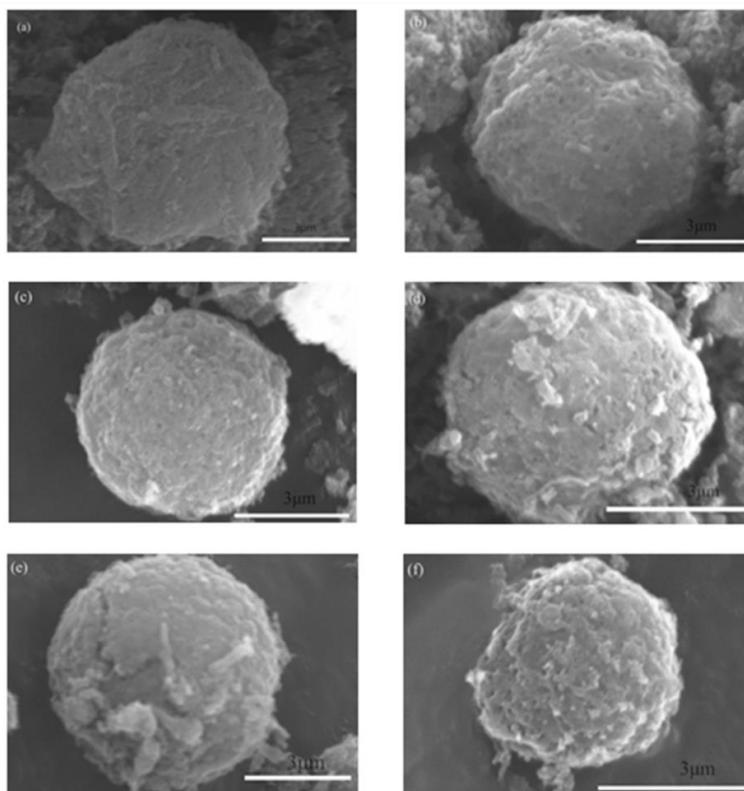


Figure 2. SEM images of the electrocatalysts N-C(a), Co-N-C-18.75(b), Co-N-C-37.5(c), Co@N-C-37.5(d), Co-N-C-56.25(e), Co-N-C-75(f)

According to SEM images (Fig. 2a-f), it can be seen that six samples, N-C (a), Co-N-C-18.75 (b), Co-N-C-37.5 (c), Co@N-C-37.5 (d), Co-N-C-56.25 (e), and Co-N-C-75 (f) have spherical morphology. Their diameter is between 5 to 10 μm . In comparison, Co-N-C-18.75(b) and Co-N-C-37.5(c) have complete spherical morphology than other electrocatalysts. This indicates that a certain amount of cobalt is beneficial to the formation of the carbon mesosphere morphology, but more cobalt content would gather in the carbon mesosphere and destroy it. To some degree, the destroyed morphology can reduce the active sites of catalysts and have a negative impact on the ORR.

The specific surface area and porosity of the electrocatalysts were calculated through N_2 isotherm adsorption/desorption. From Fig. 3(a), the results show that all catalysts have typical IV-type curves, which proves that the six catalysts have structures that are obviously mesoporous. The specific surface areas of the N-C, Co-N-C-18.75, Co-N-C-37.5, Co@N-C-37.5, Co-N-C-56.25, Co-N-C-75 catalysts were calculated, and their values were $327 \text{ m}^2 \text{ g}^{-1}$, $358 \text{ m}^2 \text{ g}^{-1}$, $419 \text{ m}^2 \text{ g}^{-1}$, $370 \text{ m}^2 \text{ g}^{-1}$, $410 \text{ m}^2 \text{ g}^{-1}$ and $357 \text{ m}^2 \text{ g}^{-1}$, respectively. According to the results, the specific surface area of the tested catalysts increases to a maximum and then decreases. With an increasing content of cobalt acetate, the specific surface area of the catalysts increases, and then decreasing when a certain amount of cobalt acetate is reached. Thus, Co-N-C-37.5 has the largest specific surface area. The reason for the increase in specific surface area is that the acetate ion could decompose to CO_2 at high temperature; the reason for the decrease in specific surface area is that the sintering of Co^{2+} at high temperature occupies the pores in the catalysts, which has a negative effect on the ORR performance. The pore size distribution was displayed in Fig. 3(b). The pore size distribution of the six catalysts was 35 and 10 nm. The pore size distribution at 35 nm is caused by etching fumed silica. The polyvinylpyrrolidone decomposes at high temperature which creates the pore size of 10 nm. In the meantime, a large number of mesopores could immensely increase the density of active sites, which would be beneficial to the ORR[17,18].

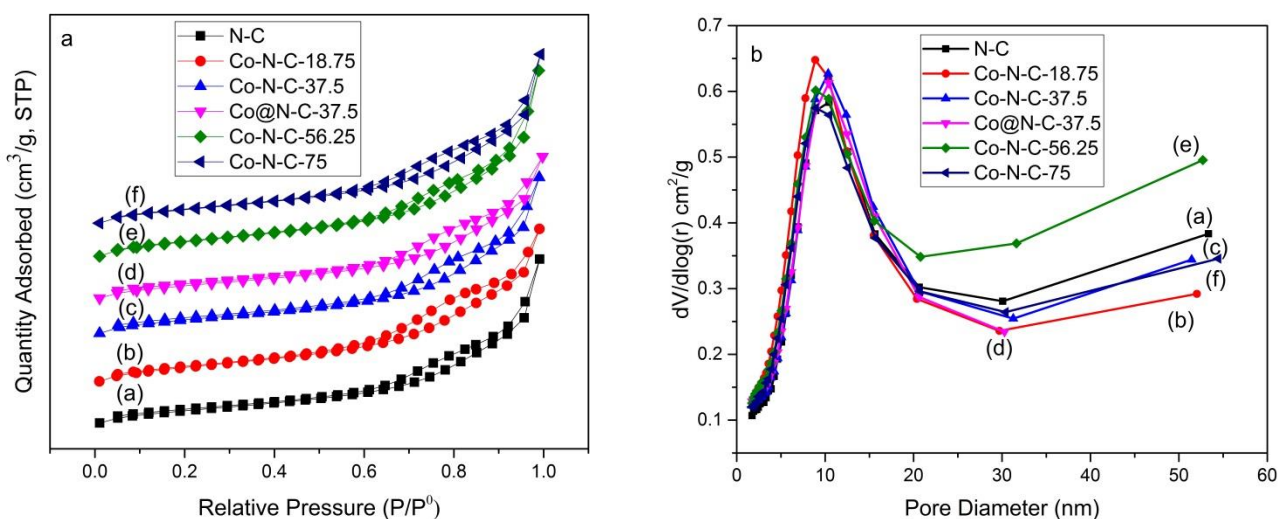


Figure 3. Nitrogen adsorption-desorption isotherms and pore-size distribution of the samples N-C (a), Co-N-C-18.75 (b), Co-N-C-37.5 (c), Co@N-C-37.5 (d), Co-N-C-56.25 (e), Co-N-C-75 (f)

XRD and Raman tests were implemented to study the modality of cobalt and carbon in the samples. XRD results were showed in Fig. 4(a). Two characteristic amorphous carbon peaks of (002) and (100) were shown in the picture. Additionally, there was no obvious peak of cobalt in the XRD results. However, according to the SEM and BET results, some cobalt nanoparticles are aggregated.

The defect degree of the catalysts was characterized by Raman test. As illustrated in the Fig.4(b), there are two peaks are found near 1350 and 1580 cm^{-1} . The peak at approximately 1350 cm^{-1} is represented by the D band and the other peak at 1580 cm^{-1} is the G band [19-21]. The ratio of the D band to the G band (I_D/I_G) indicates the defect degree of the carbon support catalysts. After calculation, the value of I_D/I_G is high, which is 2.91, 2.81, 2.78, 2.90, 2.93 and 3.35, respectively. Among them, Co-N-C-37.5 has the lowest I_D/I_G value and the highest degree of graphitization. It shows that a certain amount of cobalt is beneficial to the graphitization of the structure, but more cobalt will destroy it. Thus, Co-N-C-37.5 could have the better ORR activity.

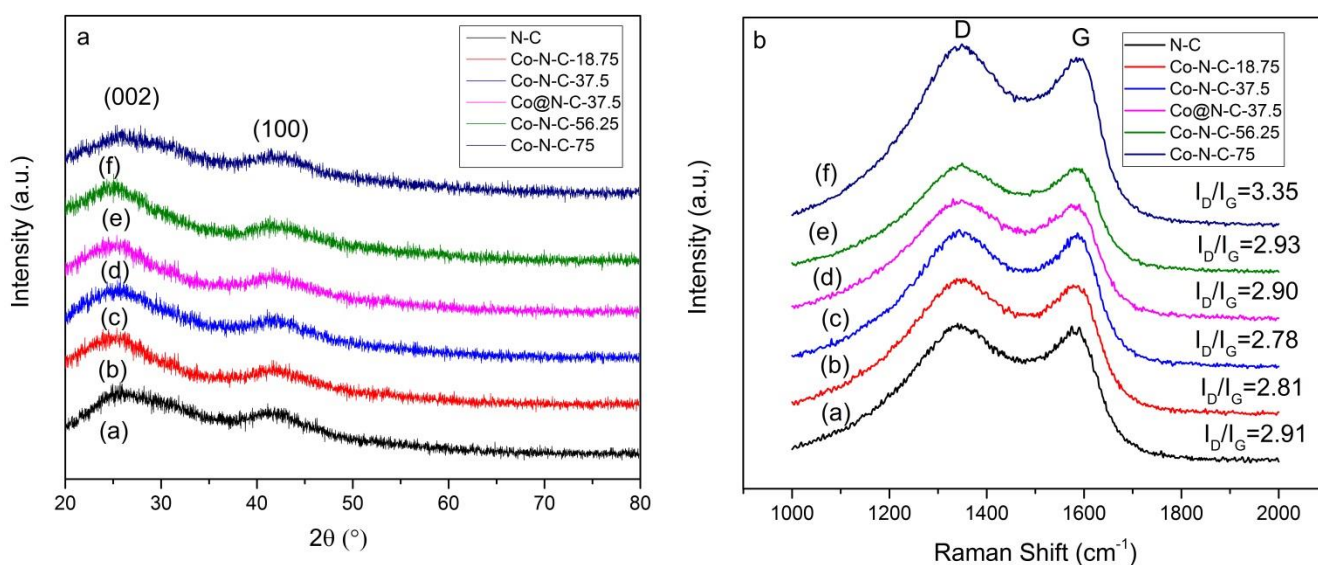


Figure 4. XRD patterns and Raman spectra of the samples N-C (a), Co-N-C-18.75 (b), Co-N-C-37.5 (c), Co@N-C-37.5 (d), Co-N-C-56.25 (e), Co-N-C-75 (f)

The valence states and elemental contents in the samples were analysed by XPS. The results were shown in Table 1 and Figs. 5-7. From Fig. 6, N1s can be divided into three peaks corresponding to pyridinic-N (398.5 eV), pyrrolic-N (399.9 eV) and graphitic-N (401.3 eV)[22]. Among the three nitrogen types, pyrrole N has lone-pair electron that binds with cobalt to promote the ORR[23]. Furthermore, a high content of pyridinic-N and graphitic-N will be beneficial for the ORR. In addition, Fig. 7 shows that the Co2p is divided into three peaks, which correspond to metallic Co (793.30 and 778.25 eV), Co-O (796.50 and 781.2 eV), Co-N (786.0 and 779.85 eV)[24,25]. Both Co-N and Co-O bonds can be beneficial for the catalytic performance of the ORR[26].

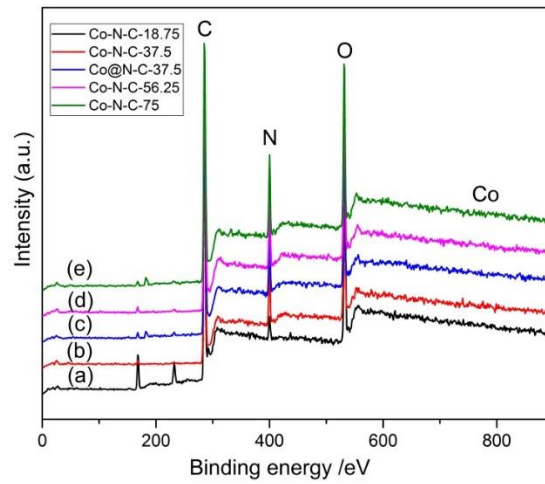


Figure 5. XPS spectra of the samples Co-N-C-18.75 (a), Co-N-C-37.5 (b), Co@N-C-37.5 (c), Co-N-C-56.25 (d), Co-N-C-75 (e)

Table 1. Elemental content of the samples

Samples	C (at%)	N (at%)	O (at%)	Co (at%)
Co-N-C-18.75	75.29	3.84	19.97	0.91
Co-N-C-37.5	69.20	11.17	18.45	1.19
Co@N-C-37.5	69.38	12.63	16.99	1.01
Co-N-C-56.25	69.78	12.22	16.73	1.28
Co-N-C-75	69.63	12.19	17.32	0.86

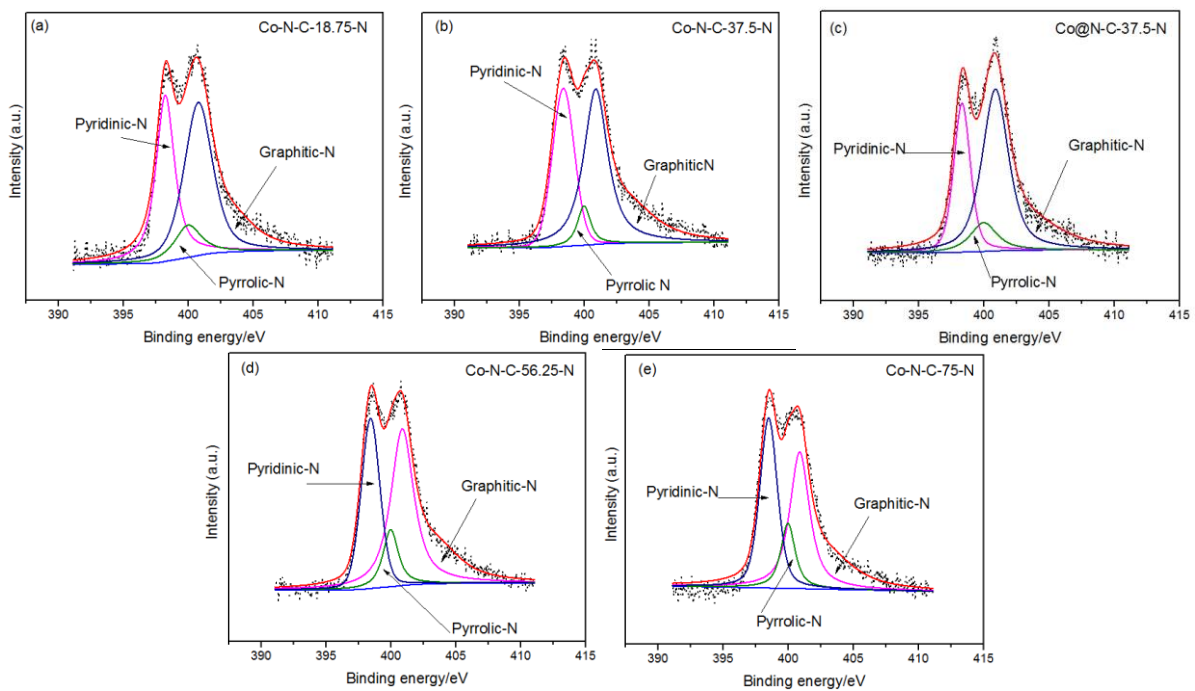


Figure 6. High-resolution N1s XPS spectra of the five samples

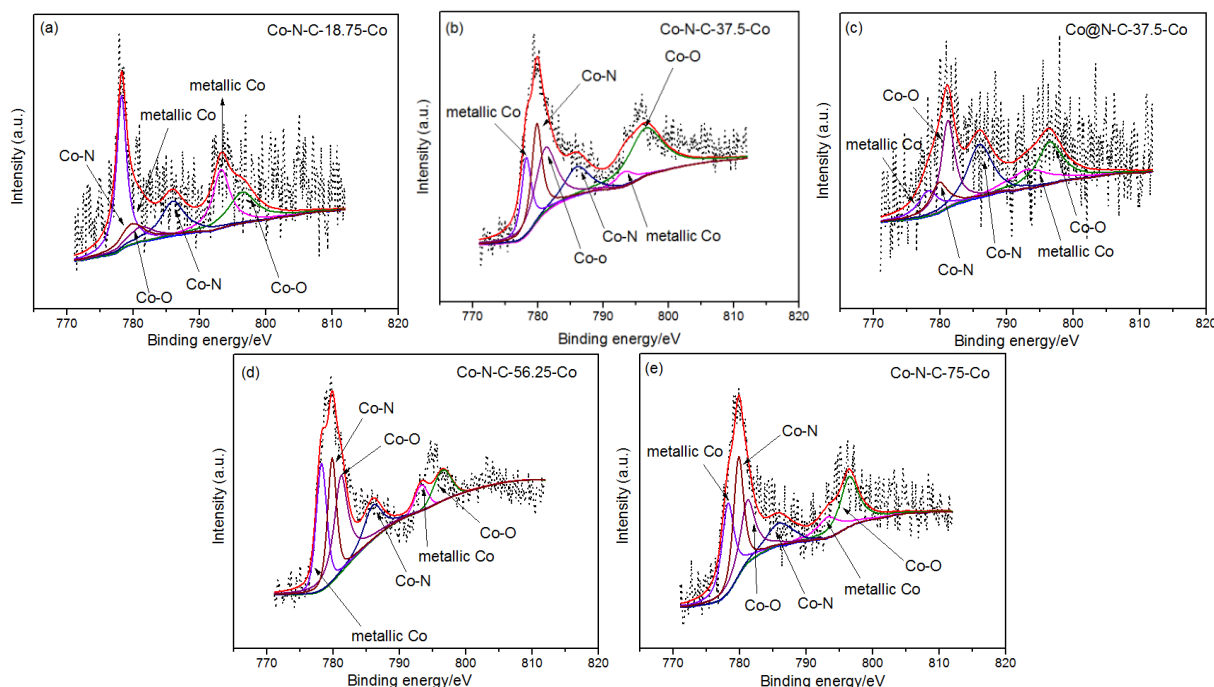


Figure 7. High-resolution Co2p XPS spectra of the five samples

Table 2. Content of different N、Co species (%) in five samples

Samples	Pyridinic-N	Pyrrolic-N	Graphitic-N	metallic Co	Co-O	Co-N
Co-N-C-18.75	35.90	10.18	53.92	44.35	29.16	26.49
Co-N-C-37.5	43.92	6.87	50.79	28.95	36.91	34.14
Co@N-C-37.5	32.84	9.96	57.20	20.95	36.87	42.18
Co-N-C-56.25	40.23	11.62	48.15	26.33	40.52	33.15
Co-N-C-75	44.91	14.56	40.53	28.98	36.20	34.82

From Table 2, it can be seen that the contents of pyridinic-N and pyrrolic-N in Co-N-C-37.5 are higher than those in the other samples. In addition, the contents of Co-N and Co-O bonds are also high. The results indicated that Co-N-C-37.5 could be a good catalyst for the ORR.

To compare the electrochemical performance of the six catalysts, a CV test was carried out. CV results are shown in Fig. 8. The CV values of catalysts are 0.766 V, 0.816 V, 0.821 V, 0.801 V, 0.796 V and 0.677 V, respectively. Among the six catalysts, Co-N-C-37.5 has the better CV peak position than other samples. The CV values of the catalysts are consistent with the conclusion of the BET and Raman analyses. It indicates that Co-N-C-37.5 could have the better ORR performance.

To further estimate the catalytic performance of the ORR, LSV was carried out. For comparison, commercial Pt/C catalysts were also tested. All the catalytic performance results for the catalysts are recorded in Table 3, Fig. 9 and Fig. 10. From Table 3 and Fig. 10, the electron transfer numbers of Co-N-C-37.5 and Co@N-C-37.5 are 4.0 and 4.3, respectively. The onset potential of Co-N-C-37.5 is higher than that of other samples and the commercial Pt/C. Additionally, the half-wave potentials of Co-N-C-37.5 and commercial Pt/C are 0.780 and 0.797 V, respectively. The difference between them is 17 mV. This indicates that Co-N-C-37.5 is a good catalyst for ORR. To compare the

ORR activity between Co-N-C-37.5 and Co-based electrocatalysts in 0.1M KOH from recent papers, the results are listed in Table 4. It can be seen that the Co-N-C-37.5 has the better ORR activity than the other electrocatalysts from recent papers in the list. It might be related to the formation and kinds of active compositions of the ORR electrocatalysts.

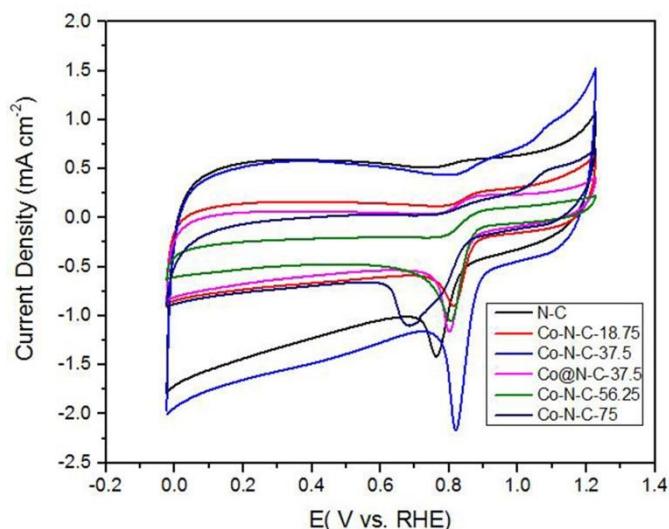
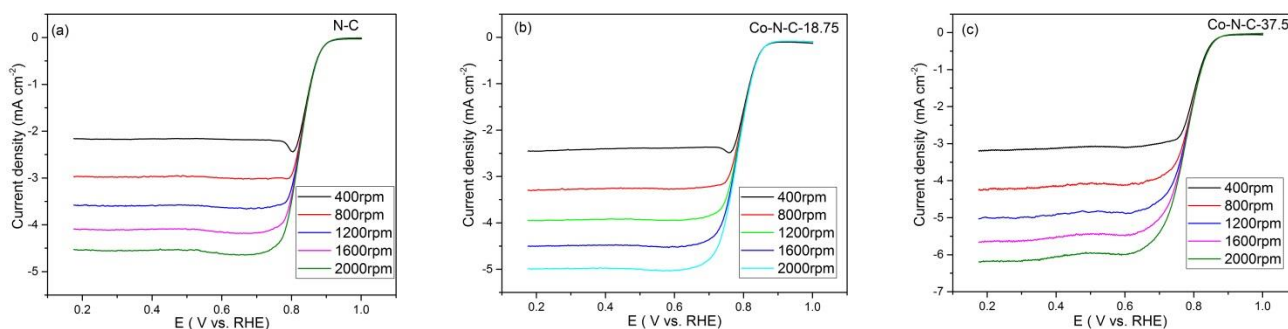


Figure 8. CV curves of N-C, Co-N-C-18.75, Co-N-C-37.5, Co@N-C-37.5, Co-N-C-56.25, Co-N-C-75 in O₂-saturated 0.1 M KOH electrolyte

Table 3. Electrocatalytic performance comparison of the samples and commercial Pt/C catalyst

Samples	Onset potential (V vs. RHE)	Half-wave potential(V vs. RHE)	Current density (mA cm ⁻²)	Electron transfer number n
N-C	0.921	0.830	4.1	3.2
Co-N-C-18.75	0.933	0.787	4.5	3.5
Co-N-C-37.5	0.979	0.780	5.6	4.0
Co@N-C-37.5	0.927	0.807	4.7	4.3
Co-N-C-56.25	0.891	0.813	4.7	3.8
Co-N-C-75	0.909	0.811	5.2	4.5
Pt/C	0.967	0.797	5.9	4.0



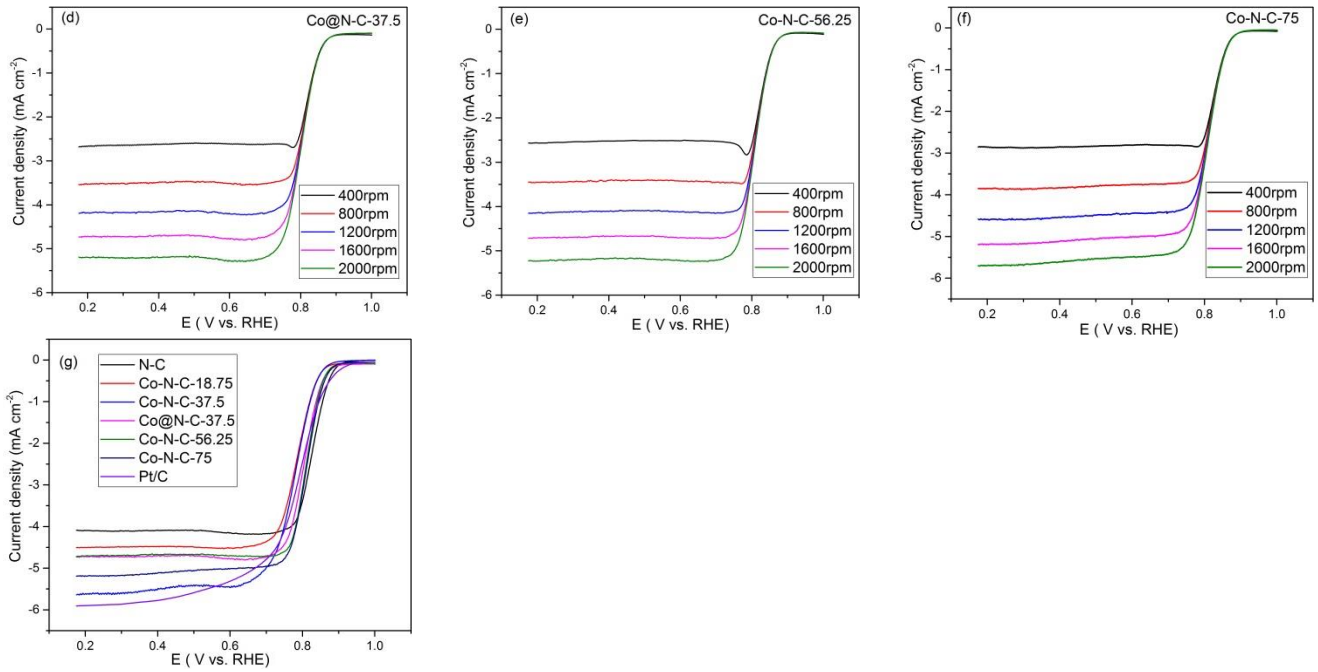
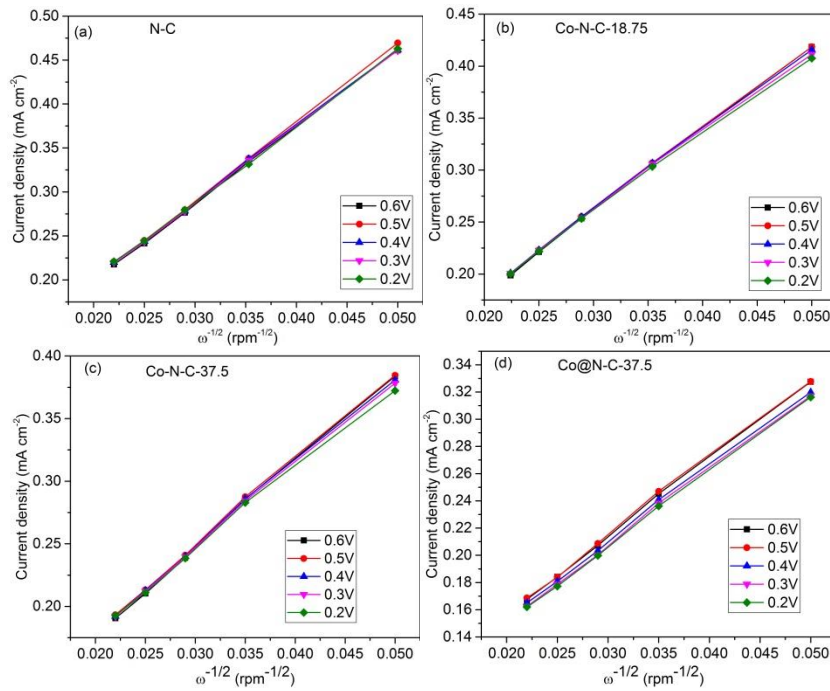


Figure 9. LSV curves and K-L plots(a-f) of the six samples in O₂ saturated 0.1 M KOH with a scan rate of 10 mV s⁻¹; (g) Six samples and Pt/C in O₂ saturated 0.1 M KOH at 1600 rpm



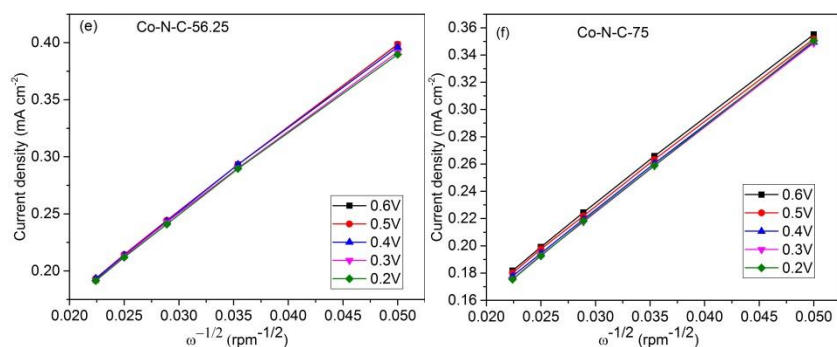


Figure 10. K-L plots(a-f) of the six samples

Table 4. Comparison of ORR activity between Co-N-C-37.5 and other Co-based catalysts from recent papers (electrocatalyst was tested at 1600 rpm in 0.1 M KOH)

Samples	Initial potential (V vs. RHE)	Half-wave potential (V vs. RHE)	References
Co-N-C-37.5	0.979^a 0.002(Ag/AgCl)	0.780^a -0.197 (Ag/AgCl)	This work
15% PANI/ZIF-67	0.85	0.75	Ref 27
N-CNF-AgNWs-Co/CoO	-0.069 (Ag/AgCl)	-0.246 (Ag/AgCl)	Ref 28
Zn/Co@C-NCNFs	-0.09 (Ag/AgCl)	-0.2 (Ag/AgCl)	Ref 29
Co-W-C/N	0.960	0.774	Ref 30
Fe-Co-N-C	0.9	0.76	Ref 31
CoP NCs	0.8	0.7	Ref 32

^aFollowing RHE potential of Co-N-C-37.5 is converted to Ag/AgCl using following Nernst equation.
 $E_{\text{Ag/AgCl}} = E(\text{vs. RHE}) - \text{pH} \times 0.059 + 0.210$

The chronoamperometric test of Co-N-C-37.5 and commercial Pt/C were conducted. Fig. 11 shows the chronoamperometric test results. As shown in Fig. 11(a), the current retention percentages of Co-N-C-37.5 in 0.1 M KOH solution is 88%, while the current retention for the commercial Pt/C is 83%. The result indicates that Co-N-C-37.5 has better stability than the commercial Pt/C in 0.1 M KOH solution. Additionally, the methanol tolerance test was carried out under the same conditions. From Fig. 11(b), the Co-N-C-37.5 catalyst exhibits better stability after adding 3 M methanol for 500 s. However, the commercial Pt/C decreased sharply under the above conditions. The test results indicate that the Co-N-C-37.5 catalyst has better stability, better methanol tolerance and a positive effect on the application of PEMFCs.

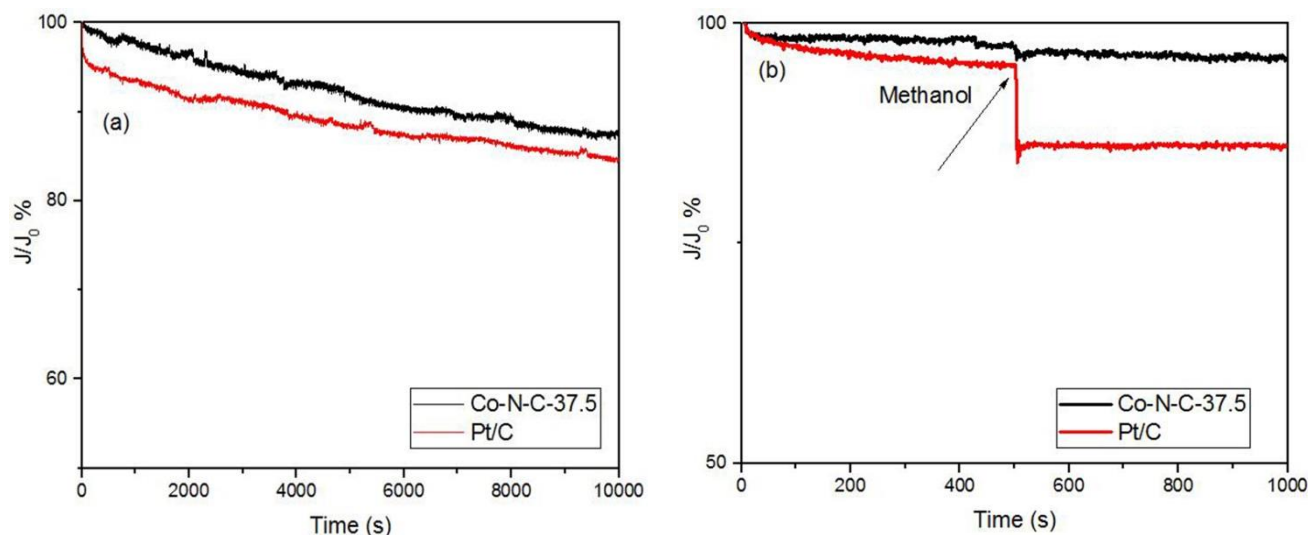


Figure 11. (a) Chronoamperometric responses of Pt/C and Co-N-C-37.5 in 0.1 M KOH ; (b) Methanol tolerance tests of Pt/C and Co-N-C-37.5 in 0.1 M KOH

4. CONCLUSIONS

In summary, cobalt (Co) and nitrogen (N) co-doped carbon sphere catalysts were successfully prepared by an electrospinning synthesis and impregnation. Then, compared the ORR performance of the commercial Pt/C with the Co, N co-doped carbon sphere catalysts. Among all catalysts, Co-N-C-37.5 has best ORR performance. The work provides an anticipated application for a novel ORR catalyst and an innovative point of view for the design and synthesis of M-N-C catalysts for many other applications, such as electrochemical sensors, lithium batteries, and supercapacitors.

ACKNOWLEDGEMENTS

This project was financially supported by the National Nature Science Foundation of China (51573090). Meanwhile, this work was also got help from Shanghai Hydrogen Technology Co., Ltd. and the State Key Laboratory of Fluorinated Functional Membrane Materials.

References

1. A. Serov, K. Artyushkova, P. Atanassov, *Adv. Energy Mater.*, 4 (2014) 919.
2. Z. Meng, S. Cai, R. Wang, H. Tang, S. Song, P. Tsiakaras, *Appl. Catal. B Environ.*, 244 (2019) 120.
3. Z. M. Cui, L. Li, A. Manthiram, J.B. Goodenough, *J. Am. Chem. Soc.*, 137 (2015) 7278.
4. G.Nam, J. Park, C. Min, P. Oh, S. Park, G.K. Min, N. Park, J. Cho, J.S. Lee, *ACS Nano*, 9 (2015) 6493.
5. J. Zhang, Z. Zhao, Z. Xia, L. Dai, *Nat. Nanotechnol.*, 10 (2015) 444.
6. X. X. Wang, V. Prabhakaran, Y. He, Y. Shao, G. Wu, *Adv. Mater.*, 31 (2019) 1805126.
7. M. Shao, Q. Chang, J.-P. Dodelet, R. Chenitz, *Chem. Rev.* 116 (2016) 3594.

8. J. Stacy, Y.N.Regmi, B.Leonard, M.-H. Fan, *Sust. Energ. Rev.*, 69 (2017) 401.
9. C.-M. Zhang, L.Hou, C.-F.Cheng, Z.-H.Zhuang, F.-Q.Zheng, W. Chen, *ChemElectroChem* , 5 (2018) 1891.
10. M. K. Debe, *Nature*, 486 (2012) 43.
11. R. Jasinski, *Nature*, 201 (1964) 1212.
12. W. F. Chen, C. H. Wang, K. Sasaki, N. Marinkovic, W. Xu, J. T. Muckerman, Y. Zhu and R. R. Adzic, *Energy Environ. Sci.*, 6 (2013) 943.
13. H. Peng, Z. Mo, S. Liao, H. Liang, L. Yang, F. Luo, H. Song, Y. Zhong , B. Zhang, *Sci. Rep.*, 3 (2013) 1765.
14. G. Wu and P. Zelenay, *Acc. Chem. Res.*, 46 (2013) 1878.
15. J. Zhang, D. He, H. Su, X. Chen, M. Pan and S. Mu, *J. Mater. Chem. A*, 2(2014) 1242.
16. H. Park, S. Oh, S. Lee, S. Choi, M. Oh, *Appl. Catal. B Environ.*, 246 (2019) 322.
17. Q. L. Zhu, W. Xia, L. R. Zheng, R. Zou, Z. Liu and Q. Xu, *ACS Energy Lett.*, 2 (2017) 504.
18. Q. Cheng, S. Han, K. Mao, C. Chen, L. Yang, Z. Zou, M. Gu, Z. Hu, H. Yang, *Nano Energy*, 52 (2018) 485.
19. E. J. Biddinger, U. S. Ozkan, *J. Phys. Chem. C*, 114 (2010) 15306.
20. N.P. Subramanian, X. Li, V. Nallathambi, S.P. Kumaraguru, H. Colon-Mercado, G. Wu, J.-W. Lee, B.N. Popov, *J. Power Sources*, 188 (2009) 38.
21. Z. Luo, S. Lim, Z. Tian, J. Shang, L. Lai, B. MacDonald, C. Fu, Z. Shen, T. Yu and J. Lin, *J. Mater. Chem.*, 21 (2011) 8038.
22. X. Chen, Z. Ning, Z. Zhou, X. Liu, J. Lei, S. Pei and Y. Zhang, *RSC Adv.*, 8 (2018) 27246.
23. M.A. Pimenta, G. Dresselhaus, M.S. Dresselhaus, L.G. Cancado, A. Jorio, R. Saito, *Phys.Chem. Chem. Phys.*, 9 (2007) 1276.
24. P. Yin, T. Yao, Y. Wu, L. Zheng, Y. Lin, W. Liu, H. Ju, J. Zhu, X. Hong, Z. Deng, G. Zhou, S. Wei, Y. Li, *Angew. Chem. Int. Ed.*, 55 (2016) 10800.
25. S. Chao, Z. Bai, Q. Cui, H. Yan, K. Wang, L. Yang, *Carbon*, 82 (2015) 77.
26. J. Wei, Y. Hu, Y. Liang, B. Kong, J. Zhang, J. Song, Q. Bao, G. P. Simon, S. P. Jiang, H. Wang, *Adv. Funct. Mater.*, 25 (2015) 5768.
27. M. Khalid, A.M.B. Honorato, H. Varela, L. Dai, *Nano Energy*, 45 (2018) 127.
28. S. Pei, Z. Zhou, X. Chen, X. Huang, T. Liu, B. Cao, F. Wang, *Int. J. Electrochem. Sci.*, 1111 (2016) 8994.
29. Q. Niu, J. Guo, B. Chen, J. Nie, X. Guo, G. Ma, *Carbon*, 114 (2017) 250.
30. S. Fu, C. Zhu, J. Song, M. H. Engelhard, B. Xiao, Dan Du, Y. Lin, *Chem. Eur J.*, 23 (2017) 10460.
31. L. Osmieri, C. Zafferoni, L. Wang, A.H.A. Monteverde Videla, A. Lavacchi, S. Specchia, *ChemElectroChem*, 5 (2018) 1954.
32. H. Yang, Y. Zhang, F. Hu, Q. Wang, *Nano Lett.*, 15 (2015) 7616.